Nanoscale

Accepted Manuscript

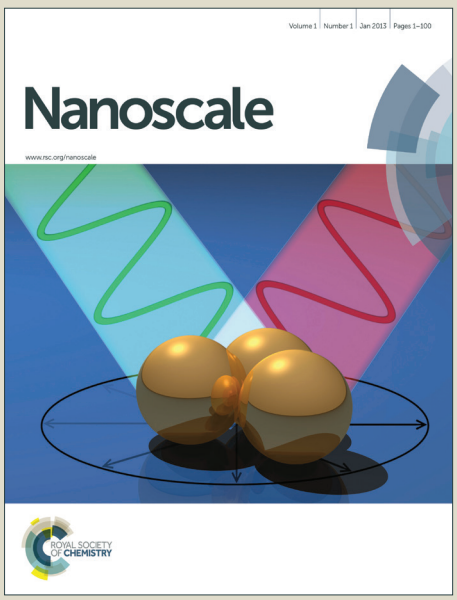

ROYAL SOCIETY OF CHEMISTRY

www.rsc.org/nanoscale

Journal Name

RSCPublishing

ARTICLE

Nano-scale displacement sensing based on van der Waals interaction

Cite this: DOI: 10.1039/xoxxoooooox

Lin Hu,[a,b] Jin Zhao,[a,b*] and Jinlong Yang[a,b*]

Received ooth January 2012,
Accepted ooth January 2012

DOI: 10.1039/xoxxoooooox

www.rsc.org/

We propose that a nano-scale displacement sensor with high resolution for weak-force systems can be realized based on vertically stacked two-dimensional (2D) atomic corrugated layer materials bound through van der Waals (vdW) interactions. Using first-principles calculations, we found that the electronic structure of bi-layer blue phosphorus (BLBP) vary appreciably with the lateral and vertical interlayer displacements. The variation of the electronic structure due to the lateral displacement is attributed to the change in the interlayer distance d_z induced by atomic layer corrugation, which is in a uniform picture with vertical displacement. Despite the different stacking configurations of BLBP, we find that the change of the in-direct band gap is proportional to d_z^{-2}. Further, this d_z^{-2} dependence is found to be applicable to other graphene-like corrugated bi-layer materials such as MoS_2. BLBP represents a large family of bi-layer 2D atomic corrugated materials for which the electronic structure is sensitive to the interlayer vertical and lateral displacement, and thus could be used for nano-scale displacement sensor. This can be done by monitoring the tunable electronic structure using absorption spectroscopy. Because this kind of sensor is established on atomic layers coupled through vdW interaction, it provides unique applications in measurements of nano-scale displacement induced by tiny external force.

Introduction

High-resolution displacement sensing is essential for scientific measurement for a wide range of applications, among which, the nano-scale positioning measurement is becoming increasingly important in ultra-precision manufacturing and metrology in nano-technological applications. On a micro-scale level, many micro-sensors such as microphones, accelerometers and pressure sensors, ultimately rely on accurately detecting small displacements with micro-scale resolution.[1-3] With the development of nanotechnology, the transducer fundamental concepts at the micro-scale are extended into the nano-scale region.[4] Nano-scale displacement sensing with high resolution has urgent applications for nano-devices.

Conventional displacement sensing are based on optical interferometry,[5] capacitance,[6] and piezoresistance.[7,8] For the nano-scale sensing, the conventional methods encounters different drawbacks. The optical methods are limited by the drawbacks of non-linearity, fringe effects, proportionality errors, volume and cost of optical components, and mostly important, the light wavelength. Capacitive sensing suffers from signal loss and is limited by area.[6] Piezoresistors scaled down to nano-scale leads to strongly increased resistance and the resistance noise followed.[7,8] To achieve high resolution, new materials, for example nanotubes, have been applied for nano-scale sensing.[4,9-13] Yet despite these attempts, it is still challenging to get high resolution for displacement induced by tiny force. For example, to measure the displacement of a quantum mechanical oscillator, a single electron transistor was applied as a displacement sensor to achieve the quantum-limited sensitivity.[1] Hence the alternative complementary methods of measuring precise displacement for weak-force system have urgent need in both scientific research and practical applications.

Vertically stacked two-dimensional (2D) layers that are stabilized by van der Waals (vdW) interactions have attracted a lot of interest recently leading to new new physical phenomena including new van Hove singularities,[14-17] Fermi velocity renormalization[18,19] and Hofstadter's butterly pattern[20-24] in

graphene bi-layer as well as the tuneable interlayer coupling in bi-layer semiconducting MoS_2.[25] In this Letter, we propose a new nano-scale displacement sensor based on bi-layer blue phosphorus (BLBP). Blue phosphorus is a new two dimensional (2D) material predicted by first principles calculations.[26] Similar to other 2D layered materials, BLBP is stabilized by vdW interactions. Using first-principles calculations within density functional theory (DFT), we found that the electronic structure of BLBP is significantly sensitive to the lateral and vertical displacement between the two layers. Both lateral and vertical displacement lead a variation of the vertical interlayer distance (d_z) which induces the change of electronic structure. In spite of the different stacking configurations, the change of the in-direct band gap is found to be proportional to d_z^{-2}. Therefore, it is expected that the nanoscale displacements can be determined by detecting the change of electronic structure using absorption spectroscopy. This proposed sensor based on vdW interactions is unique for weak-force systems.

Results and discussion

BLBP is a typical vdW bi-layer 2D system. The binding energy calculated by DFT-D2 is 25 meV/atom with a vertical interlayer distance as 3.22 Å for an A-A stacking bi-layer, which is of the same magnitude as graphene. The novelty for this bi-layer semiconductor is that the band structure significantly depends on the stacking configuration of the two BP layers. Fig.1 (b) and (c) shows the in-direct band gap (E_{gap}) and total energy change (E_{total}) when we move the top layer BP laterally into different directions while keeping the bottom layer moveless as shown in Fig.1 (a). One can see that the band gap changes significantly from 1.75 eV to 2.33 eV while as the total energy change is only within 12 meV. In Fig.1(d), we plot the energies of valence band maximum (VBM) and conduction band minimum (CBM) measured with respect to the vacuum level. It is shown that CBM is sensitive to the lateral displacement while VBM almost remains unchanged.

We chose the lateral displacement in x direction in which E_{gap} changes the most significantly to investigate the detailed electronic structure. Fig.2 (a) shows the three representative stacking configurations marked as A-A, A-B and A-B' where the upper layer moves along x direction. E_{gap} changes from 1.75 eV for A-A stacking to 2.04 eV for A-B stacking and then to 2.33 eV for A'-B stacking as shown in Fig.2(b). Consistent with Fig.1(d), the band structure shown in Fig.2 (b) confirms that the sizable band gap change is mainly induced by the change of the conduction band (CB). The valance band (VB) dispersion also varies however the energy of VBM remains unchanged. To understand this, in Fig.2 (c) we plot out the spatial probability density distribution of VBM and CBM of BLBP with different stackings. It is clearly shown that for VBM, there is almost no interlayer interaction. Yet CBM is shown to be the σ bonding state between two layers which contains significant delocalized orbital probability density in the interlayer region.

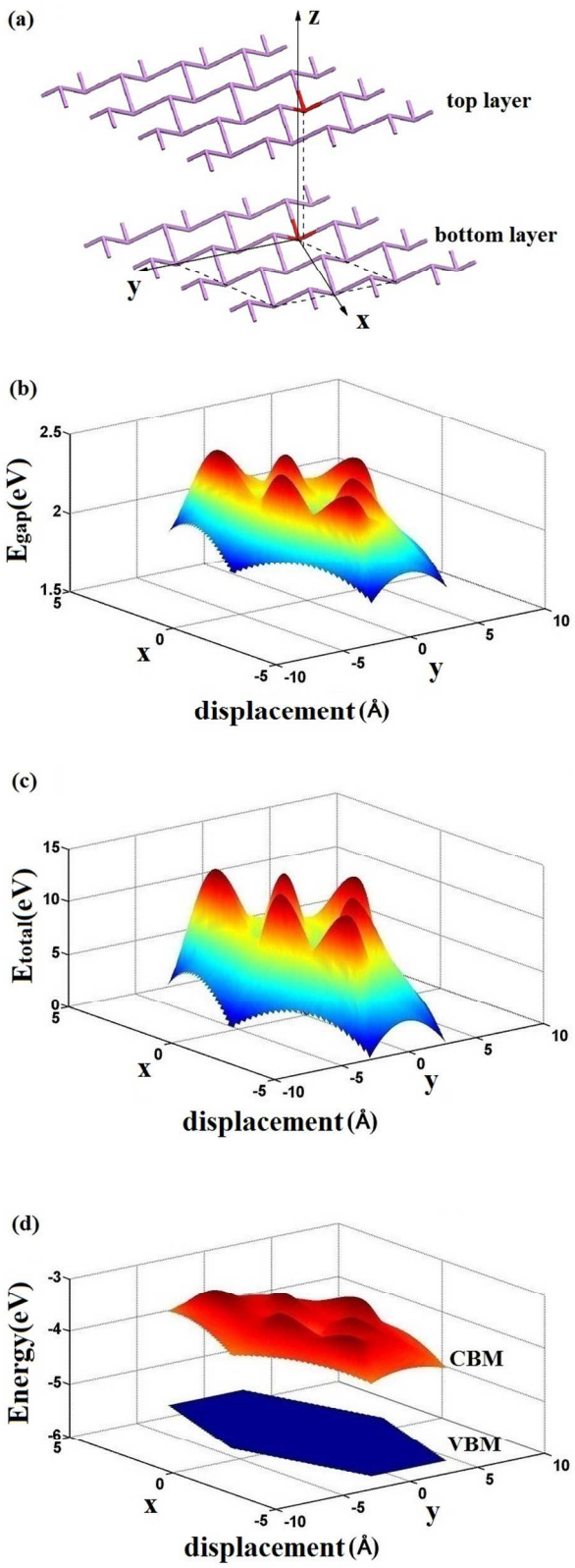

Figure 1. The BLBP electronic structure dependence on the lateral displacement. (a) The schematic diagram of lateral interlayer displacement in which the bottom layer standing still and top layer is moved laterally. (b-d) Three dimensional plotting of E_{gap}(b), E_{total} (c), E_{VBM} and E_{CBM} (d) when the top layer is moved laterally in x and y directions. For E_{VBM} and E_{CBM} the energy of vacuum level setting to zero.

The σ bonding character and delocalized probability density distribution of CBM suggest that the vertical interlayer distance d_z to be a key factor to determine the energy of CBM. In Fig.3 (a) we plot out E_{total}, CBM energy (E_{CBM}) and d_z corresponding to lateral displacement in x direction (d_x) of the top layer. One can see that E_{total}, E_{CBM} and d_z follow the same trend correlated with d_x. d_z changes remarkably from 3.2 Å for A-A stacking to 4.1 Å for A-B' stacking as shown in Fig.2 (a). The strong configuration-dependent interlayer distance can be understood due to repulsive steric effects of the corrugated atomic layers as discussed by Liu et.al..[25] The lowest energy A-A stacking has the smallest d_z because the protruding atoms in the top layer sit in the vacancies of the bottom layer resulting in reduced repulsion. For A-B' stacking the protruding atoms in top and bottom layers are face-to-face, leading to the largest repulsion and d_z.

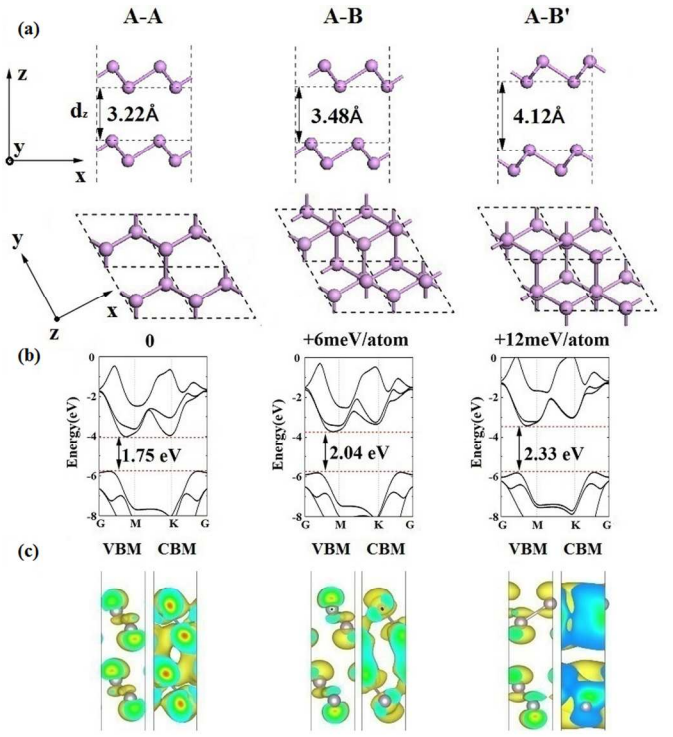

Figure 2. Atomic geometry structures (a), band structures (b) and orbital probability density distributions of VBM and CBM (c) of A-A, A-B and A-B' stacking BLBP. Corresponding E_{total}, E_{gap} and d_z are also given. The E_{total}, of A-A stacking is set to zero. For the oribital probability density distribution iso-surface plotting, the iso-value is 0.004 e/au^3.

The distinct variation of E_{CBM} with changing of d_z implies the vertical displacement may affect the electronic structure. In Fig.3 (b) we plot out E_{CBM} and E_{total} when we move the top layer BP vertically for different stacking configurations. We found that despite the different stacking configurations, E_{CBM} follows quadratic curve equation which could be fit as: $E_{CBM} = E_0 - \beta d_z^{-2}$, where E_0 and β are two parameters (The values are given in Table S1). E_0 converges to E_{CBM} for single layer BP when d_z is infinite while β is determined by the interlayer orbital hopping integral

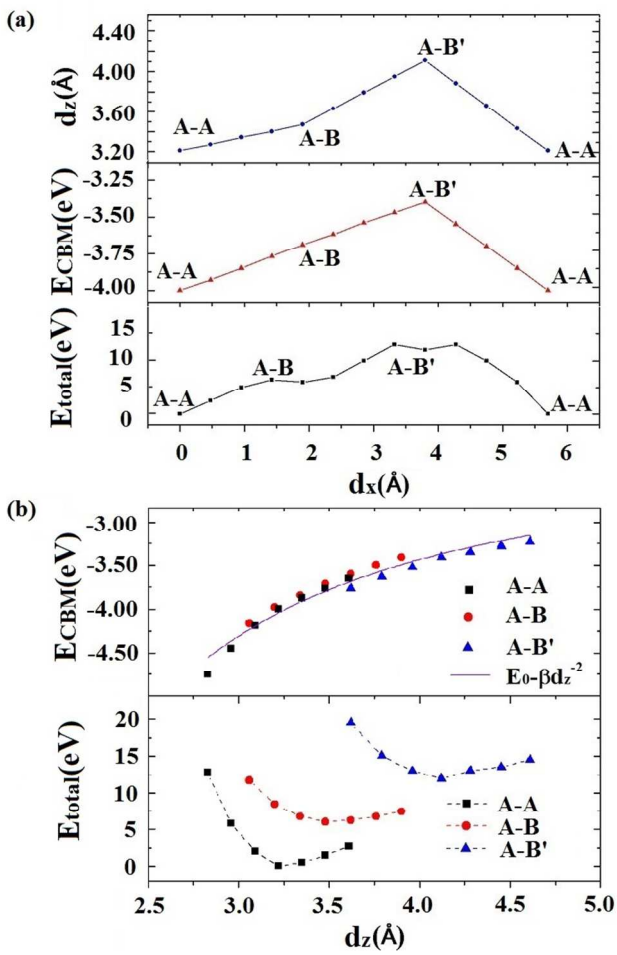

Figure 3. (a) The change of E_{total}, E_{CBM} and d_z correlated with the lateral interlayer displacement d_x on the route of A-A – A-B – A-B'– A-A. (b) The change of E_{total} and E_{CBM} correlated with d_z for the vertical interlayer displacement of A-A, A-B and A-B' stacking configurations. The fitting of $E_{CBM} = E_0 - \beta d_z^{-2}$ is also shown.

of CBM. The insensitivity of β to the stacking configuration implys that the interlayer interactions for different stacking are similar. The d_z^{-2} relationship was firstly describe by W.A. Harrison in the tight-binding model in ref.[27,28] This assumption was based on the interpretation of experimental data compared to tight-binding calculations of various systems with different constant and also was derived by comparing tight-binding bands to free-electron calculations. Later research found it works well for the free-electron-like oribitals.[29,30] The CB in BLBP shows strong non-directional delocalized interlayer probability density distribution, which leading to the good agreement with the d_z^{-2} relationship. Because the energy of VBM is constant, it is clear that E_{gap} also follows the same d_z^{-2} law with E_{CBM}. The variation of E_{CBM} and E_{gap} is as large as 1.5

eV within the vertical displacement of 1.8 Å and total energy change of 20 meV.

Because the electronic structure is very sensitive to the interlayer displacement, we propose that BLBP can be used as a nano-scale displacement sensor for weak-force systems. We provide a schematic design as shown in Fig.4 (a). During the measurement, the bottom layer is fixed while the top layer can be shifted laterally or vertically by a very weak force. The displacement is determined by measuring the electronic structure change such as photo absorption spectroscopy. Fig.4 (b) and (c) shows the calculated absorption intensity and the band structure change when the bottom layer is motionless and top layer is shifted laterally from A-A stacking to A-B' stacking. Two absorption peaks are obtained when the excitation energy is below 5 eV. Peak I at 2.75 eV that corresponds to the vertical transition from VB to CBM does not change with the top layer lateral displacement. This is because for this transition, the initial state in VB changes in the same trend with CBM as shown in Fig.4 (c). Peak II, which corresponds to the vertical excitation from VBM to CB, changes from 3.65 eV to 4.11 eV, showing significant sensitivity to top layer displacement because VBM remains constant and the final state in CB varies distinctly. (See the details of transitions I and II in supplementary materials.) Through the vertical displacement of different stacking configurations, we found that the energy of peak II (E_{PeakII}) also follows the simple d_z^{-2} trend as shown in Fig.4 (d). We propose that peak I can be used as a benchmark while the displacement could be deduced from the position of peak II. Especially, regardless of different stacking configurations, the vertical displacement could be easily obtained through the simple $E_{PeakII} \propto dz^{-2}$ relationship. In addition, the BLBP electronic structure is also sensitive to the interlayer twist angle. (see the supplementary materials) Therefore, this schematic sensor can be upgraded to a four dimensional (three dimensions plus twist angle) displacement sensor in nano-scale. In our work the band structures and absorption spectral are calculated based on DFT using HSE functional. The excitonic effects could be important for these 2D materials, we believe a further investigation using GW+BSE will be useful.[31]

We propose that this displacement sensor can be realized using different vertically stacked 2D bi-layer materials if they satisfy the following two requirements: (i) The atomic layer is corrugated so that the interlayer distance d_z changes significantly with lateral displacement and twisting. (ii) The CB or VB has significant delocalized interlayer probability density distribution. Therefore, the band structure of CB/VB changes remarkably with different d_z. We notice that analogous semiconductors as bi-layer MoS_2 and black phosphorus are found to be sensitive to the stacking configurations, which support our deduction.[25,32,33] To validate this, we have calculated the E_{gap} change versus d_z of bi-layer MoS_2 and black phosphorus when the top layer is vertically displaced as shown in Fig.5. Appreciable E_{gap} change can be observed for these three bi-layer materials. We found that E_{gap} of bi-layer MoS_2 and BLBP, which are graphene-like 2D materials, follow the unified d_z^{-2} behaviour despite different stacking configuration. For black phosphorus, since atomic structure is different and the corrugation is very large (Fig. S4), the unified d_z^{-2} dependence for different stacking configurations fails. Thus we conclude that both BLBP and bi-layer MoS_2 can be easily used to measure the d_z change since $E_{gap} \propto dz^{-2}$, however, BLBP

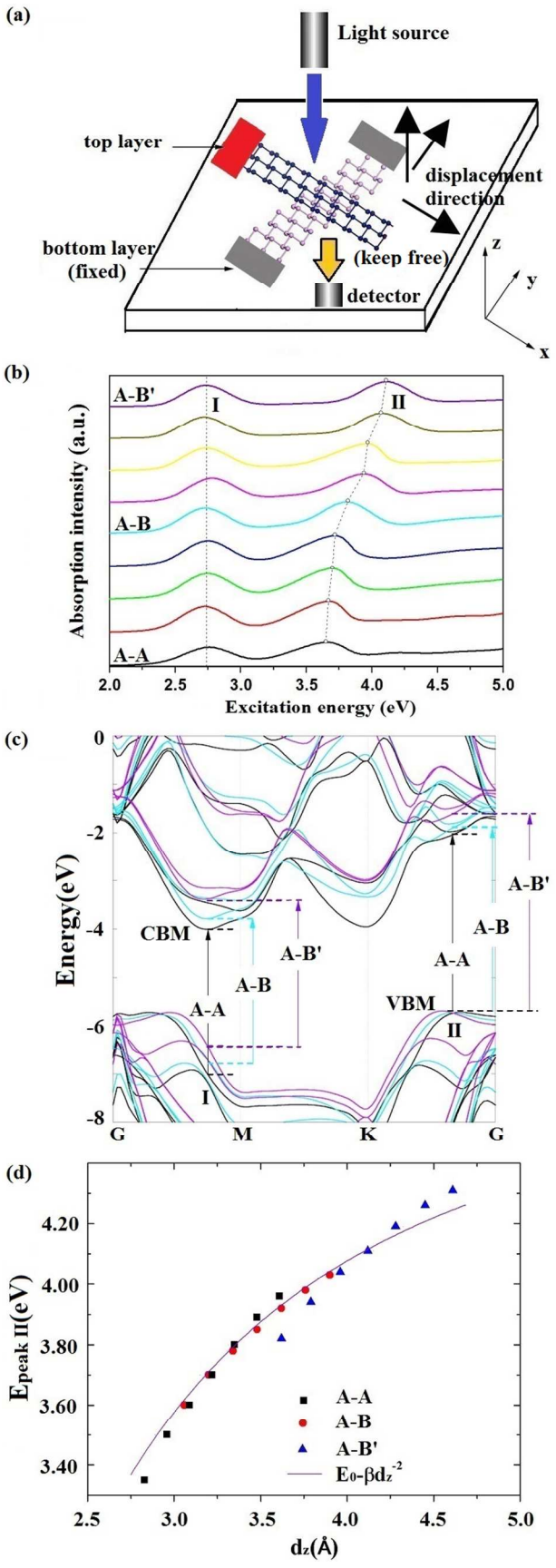

Figure 4. (a) The schematic design diagram of the nano-scale displacement sensor based on BLBP. (b-c) The absorption intensity (b) and band structure (c) of BLBP when the top layer is moved laterally from A-A (black line) through A-B (cyan line) to A-B' (purple line). (d) The change of E_{PeakII} correlated with d_z for the vertical interlayer displacement of A-A, A-B and A-B' stacking configurations. The fitting of $E_{PeakII} = E_0 - \beta d_z^{-2}$ is also shown.

has larger β value (shown in Table S1) meaning the E_{gap} tunability of BLBP is larger. Therefore we propose that BLBP is a prominent candidate as a displacement sensor for weak force system with high resolution.

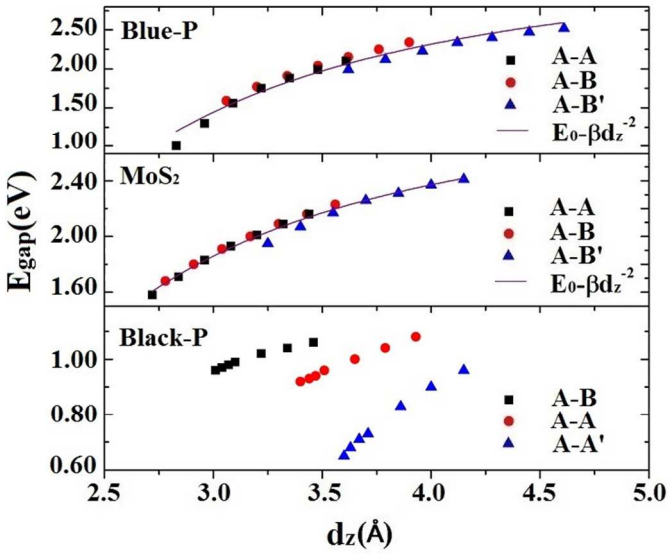

Figure 5. The change of E_{gap} with d_z for the vertical interlayer displacement of A-A, A-B and A-B' stacking configurations for BLBP, bi-layer MoS_2 and black phosphrus. For BLBP and MoS_2, the fitting of $E_{gap} = E_0 - \beta d_z^{-2}$ is also shown.

Conclusions

In summary, using first principles calculations, we found the electronic structure of BLBP coupled through vdW interaction is sensitive to the interlayer displacement. Despite the different stacking configurations, the variation of the band gap with the interlayer distance d_z follows a simple relationship $E_{gap} \propto dz^{-2}$. This simple dz^{-2} dependence is also applicable for other graphene-like corrugated bi-layer materials, for example MoS_2. Based on the tunability of electronic structure and the feasibility to measure this using photoabsorption, we propose that BLBP, as a representative of weakly coupled 2D semiconductor family, can be used as a nano-scale displacement sensor.

Computational method

First-principles calculations are performed with the Vienna Ab-initio Simulation Package (VASP).[34,35] The Perdew-Burke-Ernzerhof (GGA-PBE)[36] functional with vdW correction proposed by Grimme (DFT-D2)[37] is used in these calculations.[38,39] An energy cutoff of 600 eV is employed for

the plane wave basis sets. The projector-augmented wave (PAW)[40,41]method is used for electron-ion interaction. A vacuum spacing of about 15 Å ensures that the interactions between the layers are negligible. The dipole correction is applied to compensate the dipole interaction in the direction perpendicular to the plane. The k-point sampling uses the Monkhorst-Pack scheme[42] and employs a $11 \times 11 \times 1$ mesh. The criterion of maximum force during optimization on each atom is less than 0.01 eV/Å and the convergence criteria for energy is 10^{-5} eV. During the optimization all the atoms in both the top and bottom layers are relaxed. We scan the size of unit cell for each system to obtain the lattice parameters with the lowest energy. The spin-orbital coupling effect is included in our calculations. It is well known that DFT usually underestimated the band gap of semiconductor. To correct this problem, we chose HSE[43] functional to obtain all the electronic structure information.

Acknowledgements

This work is supported by National Key Basic Research Program (2011CB921404), by NSFC (21421063, 11322434), by CAS (XDB01020300), and by USTCSCC, SC-CAS, Tianjin, and Shanghai Supercomputer Centers. We thank Dr. Wissam A. Saidi for useful discussions.

Notes and references

[a] ICQD/Hefei National Laboratory for Physical Sciences at Microscale, and Key Laboratory of Strongly-Coupled Quantum Matter Physics, Chinese Academy of Sciences, and Department of Physics, University of Science and Technology of China, Hefei, Anhui 230026, China.

[b] Synergetic Innovation Center of Quantum Information & Quantum Physics, University of Science and Technology of China, Hefei, Anhui 230026, China.

[*] E-mail: zhaojin@ustc.edu.cn, jlyang@ustc.edu.cn

Electronic Supplementary Information (ESI) available: [details of any supplementary information available should be included here]. See DOI: 10.1039/b000000x/

1 R. G. Knobel and A. N. Cleland, Nature, 2003, 424, 291-293.
2 C. Stampfer, A. Jungen, R. Linderman, D. Obergfell, S. Roth and C. Hierold, Nano letters, 2006, 6, 1449-1453.
3 W. Suh, O. Solgaard and S. Fan, Journal of Applied Physics, 2005, 98, 033102.
4 K. C. Schwab and M. L. Roukes, Physics Today, 2005, 58, 36-42.
5 Hariharan, P. Optical Interferometry 2ndedn (San Diego: Academic Press) (2003).
6 Baxter, L. K. Capacitive Sensors: Design and Applications; IEEE Press: New York, NY, USA, 1997.
7 F. Ebrahimi, Advances in Piezoelectric Transducers, Croatia, 2011.
8 C. Smith, Physical Review, 1954, 94, 42-49.
9 C. Stampfer, T. Helbling, D. Obergfell, B. Schöberle, M. K. Tripp, A. Jungen, S. Roth, V. M. Bright and C. Hierold, Nano letters, 2006, 6, 233-237.
10 S. N. Cha, J. E. Jang, Y. Choi, G. A. J. Amaratunga, D. J. Kang, D. G. Hasko, J. E. Jung and J. M. Kim, Applied Physics Letters, 2005, 86, 083105.
11 M. Nishio, S. Sawaya, S. Akita and Y. Nakayama, Applied Physics Letters, 2005, 86, 133111.
12 H. G. Craighead, Science, 2000, 290, 1532-1535.
13 R. Lefèvre, M. Goffman, V. Derycke, C. Miko, L. Forró, J. Bourgoin and P. Hesto, Physical Review Letters, 2005, 95, 185504.
14 G. Li, A. Luican, J. M. B. Lopes dos Santos, A. H. Castro Neto, A. Reina, J. Kong and E. Y. Andrei, Nature Physics, 2009, 6, 109-113.
15 M. Yankowitz, J. Xue, D. Cormode, J. D. Sanchez-Yamagishi, K. Watanabe, T. Taniguchi, P. Jarillo-Herrero, P. Jacquod and B. J. LeRoy, Nature Physics, 2012, 8, 382-386.
16 K. Kim, S. Coh, L. Z. Tan, W. Regan, J. M. Yuk, E. Chatterjee, M. F. Crommie, M. L. Cohen, S. G. Louie and A. Zettl, Physical Review Letters, 2012, 108, 246103.
17 R. W. Havener, H. Zhuang, L. Brown, R. G. Hennig and J. Park, Nano letters, 2012, 12, 3162-3167.
18 G. Trambly de Laissardiere, D. Mayou and L. Magaud, Nano letters, 2010, 10, 804-808.
19 A. Luican, G. Li, A. Reina, J. Kong, R. R. Nair, K. S. Novoselov, A. K. Geim and E. Y. Andrei, Physical Review Letters, 2011, 106, 126802.
20 D. Hofstadter, Physical Review B, 1976, 14, 2239-2249.
21 R. Bistritzer and A. H. MacDonald, Proceedings of the National Academy of Sciences of the United States of America, 2011, 108, 12233-12237.
22 C. R. Dean, L. Wang, P. Maher, C. Forsythe, F. Ghahari, Y. Gao, J. Katoch, M. Ishigami, P. Moon, M. Koshino, T. Taniguchi, K. Watanabe, K. L. Shepard, J. Hone and P. Kim, Nature, 2013, 497, 598-602.
23 B. Hunt, J. D. Sanchez-Yamagishi, A. F. Young, M. Yankowitz, B. J. LeRoy, K. Watanabe, T. Taniguchi, P. Moon, M. Koshino, P. Jarillo-Herrero and R. C. Ashoori, Science, 2013, 340, 1427-1430.
24 L. A. Ponomarenko, R. V. Gorbachev, G. L. Yu, D. C. Elias, R. Jalil, A. A. Patel, A. Mishchenko, A. S. Mayorov, C. R. Woods, J. R. Wallbank, M. Mucha-Kruczynski, B. A. Piot, M. Potemski, I. V. Grigorieva, K. S. Novoselov, F. Guinea, V. I. Fal'ko and A. K. Geim, Nature, 2013, 497, 594-597.
25 K. Liu, L. Zhang, T. Cao, C. Jin, D. Qiu, Q. Zhou, A. Zettl, P. Yang, S. G. Louie and F. Wang, Nature communications, 2014, 5, 4966.
26 Z. Zhu and D. Tománek, Physical Review Letters, 2014, 112, 176802.
27 Harrison, W. A. Electronic Structure and Properties of Solids (Freeman, San Francisco,1980)
28 S. Froyen and W. A. Harrison, Physical Review B, 1979, 20, 2420-2422
29 A. Laref, B. Bouhafs, A. Zaoui, M. Certier and H. Aourag, Physica Status Solidi (b), 2000, 217, 911-917

30 D. Dougherty, M. Feng, H. Petek, J. T. Yates and J. Zhao, Physical Review Letters, 2012, 109, 266802
31 D. Y. Qiu, F. H. da Jornada and S. G. Louie, Physical Review Letters, 2013, 111, 216805
32 Q. Liu, L. Li, Y. Li, Z. Gao, Z. Chen and J. Lu, The Journal of Physical Chemistry C, 2012, 116, 21556-21562.
33 J. Dai and X. C. Zeng, The Journal of Physical Chemistry Letters, 2014, 5, 1289-1293.
34 G. Kresse and J. Furthmüller, Computional Materials Science, 1996, 6, 15-50.
35 G. Kresse and J. Furthmüller, Physical Review B, 1996, 54, 11169.
36 J. P. Perdew, K. Burke and M. Ernzerhof, Physical Review Letters, 1996, 77, 3865.
37 S. Grimme, Journal of computational chemistry, 2006, 27, 1787-1799.
38 S. Grimme, C. Mück-Lichtenfeld and J. Antony, The Journal of Physical Chemistry C, 2007, 111, 11199-11207.
39 S. Grimme, C. Mück-Lichtenfeld and J. Antony, Phys. Chem. Chem. Phys., 2008, 10, 3327-3334.
40 P. E. Blöchl, Physical Review B, 1994, 50, 17953-17979.
41 G. Kresse and D. Joubert, Physical Review B, 1999, 59, 1758.
42 H. J. Monkhorst and J. D. Pack, Physical Review B, 1976, 13, 5188-5192.
43 J. Heyd, G. E. Scuseria and M. Ernzerhof, The Journal of chemical physics, 2003, 118, 8207.